arXiv:1304.6890v1 [cond-mat.str-el] 25 Apr 2013

Algebraic and exponential decoherence in dissipative many-particle systems

Zi Cai and Thomas Barthel
Department of Physics and Arnold Sommerfeld Center for Theoretical Physics,
Ludwig-Maximilians-Universität München, Theresienstr. 37, 80333 Munich, Germany
(Dated: March 30, 2012)

The interplay between dissipation and many-body quantum correlations gives rise to a wealth of novel phenomena. Here we investigate spin-1/2 chains with uniform local couplings to a Markovian environment using the time-dependent density matrix renormalization group (tDMRG). For the open XXZ model, we discover that the coherence decay is algebraic instead of exponential. This is due to a vanishing gap in the spectrum of the corresponding Liouville superoperator – irrespective of the Hamiltonian gap – and can be explained on the basis of a perturbative treatment. On the contrary, decoherence in the open transverse-field Ising model is found to be always exponential. In this case, the interactions can both facilitate and impede the environment-induced decoherence.

PACS numbers: 03.65.Yz, 71.27.+a, 75.10.Pq, 75.40.Mg,

I. INTRODUCTION

If quantum systems are well-isolated from their environment, their time evolution is unitary as described by the Schrödinger equation. Ultimately though, all quantum systems are inevitably coupled to their surroundings which may fundamentally alter the static and non-equilibrium properties [1–3]. These open quantum systems provide novel perspectives for quantum many-body physics where the interplay between the many-particle correlations and dissipation gives rise to a wealth of novel phenomena, challenging both theory [4–18] and experiment [19–21]. Among the features of open quantum systems, the concept of decoherence, the dynamical destruction of quantum coherence due to interaction with an environment, is of paramount importance as it poses fundamental limitations on quantum information processing as in quantum cryptography, communication, and computation. On the other hand, one can try to exploit the effect and engineer the dissipative processes to yield desired dark states which introduces a new concept for quantum state preparation [22–25].

Decoherence has been studied extensively for small or non-interacting quantum systems. For interacting dissipative many-particle systems however, the effect of the quantum many-body correlations on the decoherence is far from being fully understood. For a given system-environment coupling, it is, for example, not clear from the outset whether interactions in the system will facilitate or impede decoherence. Recently, this problem has been addressed for a two-site Bose-Hubbard model, which can be mapped to a classical diffusion process exhibiting non-Brownian behavior and an impeding of the decoherence [11]. In this work, we use the time-dependent density matrix renormalization group (tDMRG) [26–28] to investigate the decoherence dynamics in genuine open quantum many-body systems and explain the results on the basis of an additional perturbative analysis. We focus on the problem of how the correlated many-body effects fundamentally change the decoherence dynamics and give rise to novel phenomena that are absent for the corresponding small or non-interacting systems.

Considering a spin-1/2 chain uniformly coupled to a Markovian environment, the time evolution of the system state ρ is governed by a Lindblad master equation [29] (we set $\hbar$=1)

$$\begin{aligned}\partial_t\rho &= \hat{\mathcal{L}}\rho = \hat{\mathcal{H}}\rho + \hat{\mathcal{D}}\rho \\ &= -i[H,\rho] + \gamma\sum_i\Big(L_i\rho L_i^\dagger - \frac{1}{2}\{L_i^\dagger L_i,\rho\}\Big). \quad (1)\end{aligned}$$

Here, $\hat{\mathcal{L}}$ denotes the Liouville superoperator containing two parts: $\hat{\mathcal{H}}\rho = -i[H,\rho]$ generates the evolution due to the system Hamiltonian H while the dissipative process is described by $\hat{\mathcal{D}}\rho$. L_i are the Lindblad operators describing the coupling of the system to the environment and γ quantifies the strength of this coupling. Throughout the paper we choose $L_i = S_i^z$. This type of coupling was first introduced in the study of dissipative two-state systems [30] and is widely used to describe the environment-induced decoherence. A short discussion of experimentally and technologically relevant realizations is given in section IV. Consider a single qubit (spin-1/2) in the absence of external fields ($H = 0$) that is coupled to the environment via $L_1 = S_1^z$. The master equation (1) predicts that the off-diagonal element of the qubit density matrix ρ decays exponentially with time, $\rho_{\uparrow,\downarrow}(t) \sim e^{-\gamma t/4}$, which means that superpositions of quantum states (quantum coherence) are rapidly destroyed. Below, we investigate the long-time dynamics of one or two neighboring spins

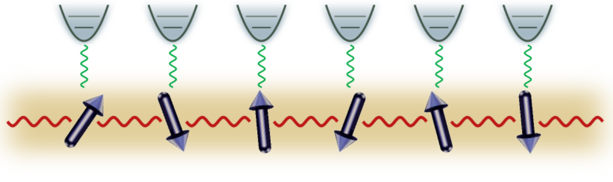

Figure 1: A quantum spin chain uniformly coupled to the environment via the z-components of the spins.

in the center of an open spin-1/2 chain. The interplay between interaction and dissipation qualitatively alters the decoherence behavior. In particular, we find (i) that, for the Heisenberg XXZ model, the coherence decay becomes algebraic instead of exponential and (ii) that, for the transverse-field Ising model, the coherence decay remains exponential but that many-body interactions can both facilitate and impede the decoherence. We explain both features on the basis of a perturbative treatment for the Liouville superoperator.

Before addressing the aforementioned specific models, some general remarks are appropriate. First, as long as $L_i^\dagger = L_i \ \forall_i$, it is easy to check that the maximally mixed state $\rho_0 \propto \mathbb{1}$ is always a steady state ($\partial_t \rho = 0$) of Eq. (1). For the models addressed in this paper, ρ_0 or restrictions of it to certain symmetry sectors are the unique steady states. Though all the initial states will eventually converge to such a steady state, the approach towards it is typically highly nontrivial and depends on the quantum many-body Hamiltonian. The dynamics (1) is governed by the non-Hermitian superoperator $\hat{\mathcal{L}}$. We denote its eigenvalues by λ_α. They have non-positive real-parts, $\operatorname{Re}\lambda_\alpha \le 0$, and the steady state has the eigenvalue $\lambda_0 = 0$. We call

$$\Delta := \min_{\alpha>0} \operatorname{Re}(-\lambda_\alpha) \tag{2}$$

the spectral gap of the Liouville operator. It can be used to characterize the long-time behavior of the system. If the gap is finite, the distance of the time-evolved state to the steady state will decrease exponentially with time, and Δ sets the corresponding inverse relaxation time. However, as we will see below, the many-body interactions in the system may qualitatively alter the dynamics by closing the gap of $\hat{\mathcal{L}}$ in the thermodynamic limit which gives rise to a novel algebraic long-time decoherence behavior.

II. ALGEBRAIC DECOHERENCE IN THE OPEN XXZ MODEL

First, let us consider the one-dimensional (1D) spin-1/2 XXZ model

$$H_{\mathrm{XXZ}} = \sum_i \left[\frac{J_{xy}}{2} (S_i^+ S_{i+1}^- + S_i^- S_{i+1}^+) + J_z S_i^z S_{i+1}^z \right] \tag{3}$$

uniformly coupled to the environment via the z-components of the spins, $L_i = S_i^z$. We study the time evolution of the system density matrix $\rho(t)$ based on the master equation (1) with the initial state $\rho(0) = |\Psi_0\rangle\langle\Psi_0|$ being the Néel state $|\Psi_0\rangle = |\uparrow\downarrow \cdots \uparrow\downarrow\rangle$. In the absence of dissipation ($\gamma = 0$), the time evolution for this setup has for example been studied in the context of quantum quenches [31–33], where the long-time behavior highly depends on J_z/J_{xy}. In this model, the total magnetization $\sum_i S_i^z$ is conserved. As a consequence, the off-diagonal element $\rho^i_{\uparrow,\downarrow} = \langle S_i^+ \rangle$ of the single-site density matrices are strictly zero for all times and can not be used to monitor the decoherence. Instead, we choose the off-diagonal term $C = \langle S_i^+ S_{i+1}^- \rangle$ of the two-site density matrix to quantify the decoherence, where sites i and $i+1$ are located in the center of the chain. For the simplest case of a two-site system ($N = 2$), it is easy to show that, in the subspace of zero magnetization, the model can be mapped to the decoherence problem of a single spin subject to a transverse field and that the off-diagonal element of the reduced density matrix decays exponentially (see appendix B).

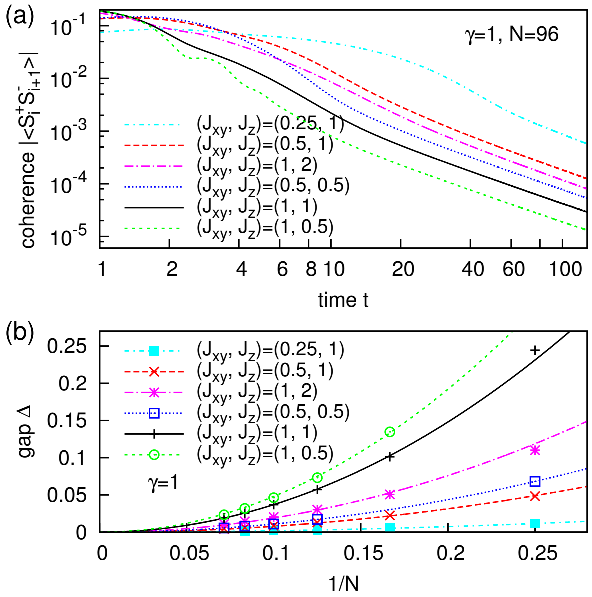

Figure 2: (a) Power-law decay of the off-diagonal density matrix element $C = \langle S_i^+ S_{i+1}^- \rangle$ in the dissipative XXZ chain (3) of length $N = 96$ for different J_{xy}, J_z and fixed bath coupling $\gamma = 1$, evaluated in the center of the chain. (b) Finite-size scaling of the gap (2) of the Liouville superoperator $\hat{\mathcal{L}}$ for the open XXZ model, obtained by exact diagonalization (ED).

In order to study the effects of the many-body correlations on the decoherence, we employ tDMRG [26–28]. As shown in Ref. [34], the propagator $\exp(\hat{\mathcal{L}}t)$ can be approximated by a circuit of two-site gates with an accuracy that is well-controlled in terms of the operationally relevant $(1 \to 1)$-norm. Here, we specifically employ a fourth-order Trotter-Suzuki decomposition with a time-step of size $\Delta t = 0.125$. Starting from certain product states $\rho(0)$, the time-evolved states are obtained by applying the local Trotter gates and approximating $\rho(t)$ by matrix product states (MPS) [35–37]. The essence of the DMRG procedure is to express $\rho(t)$ in every step of the simulation in a reduced Hilbert-Schmidt orthonormal operator basis $\{O_i^L \otimes O_i^R\}$ for a spatial splitting of the system into a left and a right part so that $\rho(t) = \sum_i \nu_i O_i^L \otimes O_i^R$. Such a representation can always be obtained by singular value decomposition. The approximation consists in discarding all components i with weights $\nu_i^2 / \sum_j \nu_j^2$ below a certain threshold ϵ (between

10^{-10} and 10^{-12} in this work). One has to ensure convergence of the numerical results with respect to the truncation threshold ϵ and the system size N in order to capture the physics of the thermodynamic limit. This is carried out in appendix C.

The evolution of the coherence $C(t)$ in open XXZ chains is shown in Fig. 2. In the long-time limit, we find the coherence to decay algebraically, instead of exponentially, according to the power-law

$$C(t) \propto t^{-\eta} \quad \text{with} \quad \eta \approx 1.58. \tag{4}$$

The exponent η is in the studied parameter regime independent of the system parameters J_{xy}, J_z, and γ. In general, an algebraic decay implies the absence of a characteristic time scale in the long-time dynamics. It results from the vanishing of the gap Δ of the Liouvillian $\hat{\mathcal{L}}$ in the thermodynamic limit. That this is indeed the case can be verified numerically by exact diagonalization as shown in Fig. 2b.

To get a better understanding for the vanishing of the gap Δ, let us perform a second order perturbative analysis to derive an effective superexchange Liouvillian $\hat{\mathcal{L}}_{\text{eff}}$ for the limit $\gamma \gg |J_z|, |J_{xy}|$ of strong dissipation. The Liouvillian can be split into an unperturbed part $\hat{\mathcal{L}}_0\rho := -i[H_z, \rho] + \hat{\mathcal{D}}\rho$, where $H_z = J_z \sum_i S_i^z S_{i+1}^z$, and the perturbation $\hat{\mathcal{L}}_1\rho := -i[H_{xy}, \rho]$ with $H_{xy} = \frac{J_{xy}}{2}\sum_i (S_i^+ S_{i+1}^- + S_i^- S_{i+1}^+)$. The steady states of $\hat{\mathcal{L}}_0$ (eigenvalue $\lambda_0 = 0$) are $\rho_0^{\boldsymbol{\sigma}} = |\boldsymbol{\sigma}\rangle\langle\boldsymbol{\sigma}|$, where $|\boldsymbol{\sigma}\rangle = |\sigma_1 \ldots \sigma_N\rangle$ are the $\{S_i^z\}$-eigenstates spanning the Hilbert space of the spin configurations with zero total magnetization. The effect of a small coupling J_{xy} is to lift the degeneracy in the steady state manifold through a superexchange process which leads us to an effective Liouvillian $\hat{\mathcal{L}}_{\text{eff}}$, constrained to the subspace $\mathbb{H}$ spanned by the operators $\rho_0^{\boldsymbol{\sigma}}$. $\mathbb{H}$ is to be understood as a subspace of the vector space $\mathcal{B}(\mathscr{H})$ of linear operators on the Hilbert space $\mathscr{H}$, i.e., $\hat{\mathcal{L}} : \mathcal{B}(\mathscr{H}) \to \mathcal{B}(\mathscr{H})$ and $\hat{\mathcal{L}}_{\text{eff}} : \mathbb{H} \to \mathbb{H}$. One obtains

$$\hat{\mathcal{L}}_{\text{eff}} = \hat{\mathcal{P}}\hat{\mathcal{L}}_1 \frac{1}{\lambda_0 - \hat{\mathcal{L}}_0} \hat{\mathcal{L}}_1 \hat{\mathcal{P}}. \tag{5}$$

$\hat{\mathcal{P}}$ is the projector onto the subspace $\mathbb{H}$. The intermediate states in the perturbation theory are of the form $\Lambda_1^{\boldsymbol{\sigma}\boldsymbol{\sigma}'} = |\boldsymbol{\sigma}\rangle\langle\boldsymbol{\sigma}'|$, where $|\boldsymbol{\sigma}'\rangle = (S_i^+ S_{i+1}^- + S_i^- S_{i+1}^+)|\boldsymbol{\sigma}\rangle$ for some bond $(i, i+1)$. Their $\hat{\mathcal{L}}_0$-eigenvalues, needed to evaluate the denominator in Eq. (5), are $-\gamma$ or $-\gamma \pm iJ_z$, depending on $\boldsymbol{\sigma}$. However, the term $\pm iJ_z$ can be ignored as it represents an irrelevant contribution of order $1/\gamma^2$ to $\hat{\mathcal{L}}_{\text{eff}}$. The full calculation given in appendix A 1 shows that the matrix elements of the effective Liouvillian are identical with those of the ferromagnetic Heisenberg model

$$H_{\text{eff}} = \frac{-J_{xy}^2}{\gamma} \sum_i \left[\frac{1}{2}(S_i^+ S_{i+1}^- + S_i^- S_{i+1}^-) + S_i^z S_{i+1}^z - \frac{1}{4}\right] \tag{6}$$

in the sense that

$$\hat{\mathcal{L}}_{\text{eff}}|\boldsymbol{\sigma}\rangle\langle\boldsymbol{\sigma}| = -\sum_{\boldsymbol{\sigma}'} \langle\boldsymbol{\sigma}'|H_{\text{eff}}|\boldsymbol{\sigma}\rangle \cdot |\boldsymbol{\sigma}'\rangle\langle\boldsymbol{\sigma}'|. \tag{7}$$

As a consequence, at the level of the second order perturbation theory, the gap (2) of the effective Liouvillian $\hat{\mathcal{L}}_{\text{eff}}$ is that of the Heisenberg ferromagnet H_{eff}. Its gap vanishes as $1/N^2$ due to the quadratic spin-wave dispersion around zero momentum and the $2\pi/N$ spacing of the quasi-momenta. This explains the quadratic behavior of the gaps Δ for the full model in Fig. 2b.

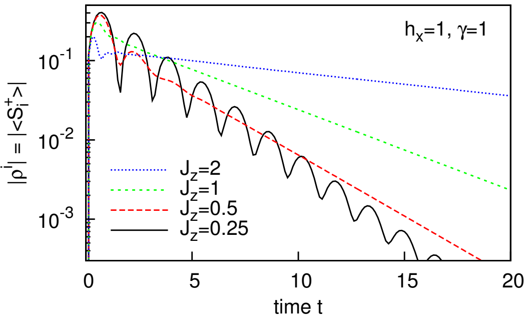

Figure 3: Time evolution of $|\rho^i_{\uparrow,\downarrow}(t)|$ for the dissipative transverse-field Ising model (8) with different J_z, fixed bath coupling $\gamma = 1$, field $h_x = 1$, and system size $N = 64$.

III. DECOHERENCE IN THE OPEN TRANSVERSE ISING MODEL

A second paradigmatic example is the dissipative transverse-field Ising model

$$\begin{aligned} H_{\text{TI}} &= \sum_i (J_z \sigma_i^z \sigma_{i+1}^z - h_x \sigma_i^x) \\ &= \sum_i (4 J_z S_i^z S_{i+1}^z - 2 h_x S_i^x) \end{aligned} \tag{8}$$

with the interaction strength J_z, the transverse magnetic field h_x, and the Pauli matrices σ_i^α. To study the interplay of interaction and dissipation, we set for simplicity $h_x = 1$ and vary J_z and the bath coupling γ. As Lindblad operators, we choose again $L_i = S_i^z$ and study the time evolution of the system density matrix based on Eq. (1) starting from a fully polarized state, i.e., $\rho(0) = |\Psi_0'\rangle\langle\Psi_0'|$ with $|\Psi_0'\rangle = |\uparrow\uparrow \cdots \uparrow\uparrow\rangle$. Alternative initial states have also been checked. However, as we are foremost interested in the long-time behavior, the choice of the initial state is of minor importance. Let us first consider the noninteracting case with $J_z = 0$ which reduces to the decoherence problem of a single spin subject to an external field. In this case, the off-diagonal element $\rho^i_{\uparrow,\downarrow} = \langle S_i^+\rangle$ of the single-site reduced density matrix decays exponentially in the long-time limit as $\rho^i_{\uparrow,\downarrow}(t) \sim e^{-\Delta_0 t}$, where the decay rate is $\Delta_0 = \gamma/4$ (as long as $\gamma \le 8|h_x|$; see appendix B). For the interacting many-body system, one

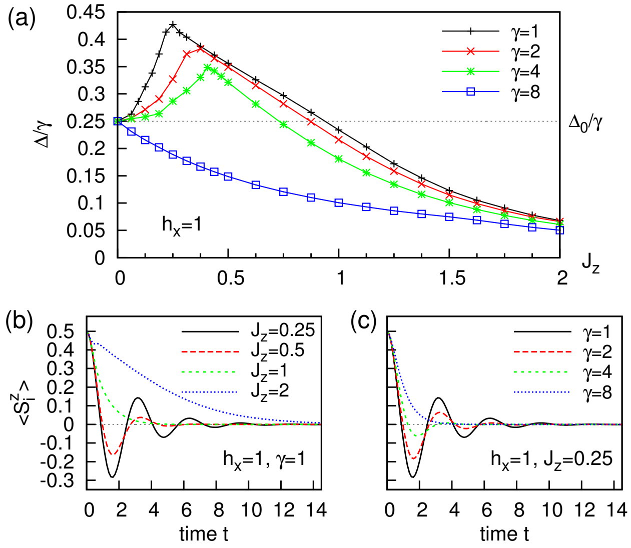

Figure 4: (a) The renormalized decoherence rate Δ/γ [Eq. (9)] for the dissipative transverse Ising model (8) as a function of J_z for different bath couplings γ. (b) Time evolution of the magnetization $\langle S_i^z \rangle$ for fixed $\gamma = 1$ and different J_z, where site i is in the middle of the chain. (c) Dynamics of $\langle S_i^z \rangle$ for fixed $J_z = 0.25$ and different γ. In all cases the system contained $N = 64$ sites.

can use $|\rho^i_{\uparrow,\downarrow}(t)|$, with site i in the middle of the chain, to monitor the coherence decay. In contrast to the situation for the open XXZ model, we find that in the long-time limit the coherence always decreases exponentially

$$|\rho^i_{\uparrow,\downarrow}(t)| \sim e^{-\Delta t}, \tag{9}$$

where the decoherence rate (inverse relaxation time) Δ is determined by the interplay of interaction and dissipation.

The evolution of $|\rho^i_{\uparrow,\downarrow}(t)|$ for different J_z and fixed bath coupling $\gamma = 1$ is shown in Fig. 3. For small J_z, the decoherence dynamics is well described by oscillations of exponentially decaying amplitude. For large J_z, $|\rho^i_{\uparrow,\downarrow}(t)|$ decays exponentially without oscillations. Similar behavior was found in the relaxation dynamics of the quenched 1D XXZ model without dissipation [31–33]. Now we turn to the question of whether the interaction facilitates or impedes the decoherence. In other words, the question is whether the decoherence rate Δ is below or above that of the noninteracting case $J_z = 0$ with $\Delta_0 = \gamma/4$. As shown in Fig. 4a, the answer to this question depends in an intricate manner on the values of γ and J_z. In the presence of weak dissipation (small γ), the dependence of Δ on J_z is non-monotonic. The interaction facilitates the environment-induced decoherence ($\Delta > \Delta_0$) for small J_z, while it impedes the decoherence ($\Delta < \Delta_0$) for large J_z. For sufficiently strong dissipation, the interaction always suppresses the decoherence.

In order to obtain a better understanding of the fact that interaction and dissipation cooperate to enhance the decoherence in the case of small J_z and γ, we calculate the dynamics of the magnetization $\langle S_i^z \rangle$ for different J_z and γ, as shown in Figures 4b and 4c. For small J_z and γ, $\langle S_i^z \rangle$ is well described by an exponentially decaying oscillation. Generally, for open many-body systems, the long-range quantum correlations are usually destroyed during the long-time dissipative dynamics. As a consequence, the quantum entanglement between a single spin and the rest of the system is weak. This allows us to explain the above observations in a mean-field framework corresponding to the decoupling of the interaction term $S_i^z S_{i+1}^z \sim S_i^z \langle S^z \rangle$. On a qualitative level, the decoherence in the long-time limit can be understood as that of a single spin in a constant transverse field and a longitudinal field $2\langle S^z(t) \rangle$ due to its nearest neighbors. Figures 4b and 4c show that, for small J_z and γ, the longitudinal field $\langle S^z(t) \rangle$ is quickly oscillating – hence, playing a role similar to that of noise and thus accelerating the decoherence. Once, the oscillations of $\langle S^z(t) \rangle$ vanish (large J_z or γ), the decoherence is suppressed.

The second key observation, that strong interaction impedes the decoherence, can again be understood on the basis of a perturbative analysis, here in the limit of a weak magnetic field, $\gamma \gg |h_x|$. The field terms $\propto h_x$ of the Liouvillian are considered as a perturbation so that $\hat{\mathcal{L}} = \hat{\mathcal{L}}_0 + \hat{\mathcal{L}}_1$ with

$$\hat{\mathcal{L}}_0 \rho = -i[H_z, \rho] + \hat{\mathcal{D}}\rho \quad \text{and} \quad \hat{\mathcal{L}}_1 \rho = -i[H_x, \rho], \tag{10}$$

where $H_z = 4J_z \sum_i S_i^z S_{i+1}^z$ and $H_x = -2h_x \sum_i S_i^x$. In the second order perturbation theory, the eigenoperators of $\hat{\mathcal{L}}_0$ are similar to those in the treatment of the open XXZ model (now, the dynamics is not constrained to sectors of constant magnetization), but the intermediate states are different. Their $\hat{\mathcal{L}}_0$-eigenvalues are $-\gamma/2$ and $-\gamma/2 \pm i4J_z$. The effective Liouville superoperator (5) is again of the form (7) and the effective Hamiltonian reads

$$H_{\text{eff}} = \sum_i \left[\frac{\alpha + \alpha'}{4} - (\alpha - \alpha') S_{i-1}^z S_{i+1}^z \right] \left(\frac{1}{2} - S_i^x \right) \tag{11}$$

in this case, where $\alpha = 16h_x^2/\gamma$ and $\alpha' = 4h_x^2\gamma/(\gamma^2/4 + (4J_z)^2)$. Based on Eq. (11), one can show that the gap (2) of the effective Liouvillian has for small J_z a value $\lesssim (\alpha + \alpha')/4$. For sufficiently large J_z, the gap is given by α'. The corresponding eigenstate of H_{eff} is the spin-wave-like state $\sum_j |\uparrow^x \cdots \uparrow^x \downarrow_j^x \downarrow_{j+1}^x \uparrow^x \cdots \uparrow^x\rangle$, where $S_i^x |\uparrow_i^x\rangle = \frac{1}{2} |\uparrow_i^x\rangle$. A detailed derivation is given in appendix A 2. So the gap decays as $1/J_z^2$, i.e., strong interaction impedes decoherence as we have found in the quasi-exact numerical analysis.

IV. EXPERIMENTAL REALIZATIONS AND APPLICATIONS

Besides being of fundamental theoretical interest, the two dissipative models addressed in this paper are of broad experimental and technological relevance. We shortly mention a few examples. A uniform coupling to the environment via Lindblad operators $L_i = S_i^z$ occurs for example naturally in quantum computer architectures [38, 39] based on superconducting flux qubits (rf-SQUIDs) through fluctuations of the external magnetic flux [40–42]. Inductive coupling of flux qubits yields the Ising-type interaction $S_i^z S_j^z$ [43–45]. In ultracold atom systems [46] where both interaction and dissipation can be controlled, the corresponding Lindblad operators $L_i = n_i$ describe laser fluctuations and incoherent scattering of the laser light [47–49]. With quantum dot spin-qubits [50, 51] one can implement both, the transverse Ising model [52] and the Heisenberg model [50], where $L_i = S_i^z$ describes the effect of variations in the longitudinal nuclear magnetic field.

V. CONCLUSION

In summary, we have studied the long-time dynamics of open quantum spin systems, discovering that the quantum many-body effects can significantly change the nature of the environment-induced decoherence by either altering the exponential coherence decay to being algebraic or, alternatively, by increasing or decreasing the decay rate. Besides illustrative quasi-exact tDMRG simulations, we have explained those effects by a perturbative analysis. Another interesting direction for further investigations are driven-dissipative quantum many-body systems, where external force drives the system far from equilibrium and the interplay between driving, dissipation, and interaction may give rise to further novel non-equilibrium phenomena.

Acknowledgments

We gratefully acknowledge discussions with U. Schollwöck and funding by the German Research Foundation through DFG FOR 801.

Appendix A: Perturbative treatment

1. Open spin-1/2 XXZ model with $L_i = S_i^z$

Let us again consider the spin-1/2 XXZ model (3) coupled to a Markovian environment according to the Lindblad master equation (1) with uniform Lindblad operators $L_i = S_i^z$ and bath coupling strength γ. Based on a perturbative treatment, one can derive an effective Liouville superoperator $\hat{\mathcal{L}}_{\text{eff}}$ for the limit of strong bath coupling $\gamma \gg |J_{xy}|, |J_z|$. To this purpose, the Liouvillian is split into an unperturbed part $\hat{\mathcal{L}}_0$ and a perturbation $\hat{\mathcal{L}}_1$ such that

$$\hat{\mathcal{L}} = \hat{\mathcal{L}}_0 + \hat{\mathcal{L}}_1, \tag{A1}$$

$$\hat{\mathcal{L}}_0\rho = -i[H_z, \rho] + \gamma \sum_i (S_i^z \rho S_i^z - \rho/4), \tag{A2}$$

$$\hat{\mathcal{L}}_1\rho = -i[H_{xy}, \rho], \tag{A3}$$

where $H_z = J_z \sum_i S_i^z S_{i+1}^z$ and $H_{xy} = \frac{J_{xy}}{2}\sum_i (S_i^+ S_{i+1}^- + S_i^- S_{i+1}^+)$ as in Eq. (3). The Liouvillian conserves the total magnetization such that $[\sum_i S_i^z, \rho(t)] = 0\ \forall_t$. As in the main part of the paper, we choose the symmetry sector of zero magnetization for the following.

The steady states (eigenvalue $\lambda_0 = 0$) of the unperturbed part $\hat{\mathcal{L}}_0$ are of the form $\rho_0^{\boldsymbol{\sigma}} := |\boldsymbol{\sigma}\rangle\langle\boldsymbol{\sigma}|$ with $\{S_i^z\}$-eigenstates $|\boldsymbol{\sigma}\rangle = |\sigma_1 \ldots \sigma_N\rangle$ obeying $S_i^z|\boldsymbol{\sigma}\rangle = \frac{\sigma_i}{2}|\boldsymbol{\sigma}\rangle$. Within the second order perturbation theory, the resulting effective Liouvillian is given by Eq. (5) with $\hat{\mathcal{P}}$ projecting onto the space $\mathbb{H}$, spanned by the unperturbed steady states $\rho_0^{\boldsymbol{\sigma}}$. Starting from such a state, the intermediate states (after application of $\hat{\mathcal{L}}_1$) are of the form $\Lambda^{\boldsymbol{\sigma}\boldsymbol{\sigma}'} := |\boldsymbol{\sigma}\rangle\langle\boldsymbol{\sigma}'|$ such that $|\boldsymbol{\sigma}'\rangle = (S_i^+ S_{i+1}^- + S_i^- S_{i+1}^+)|\boldsymbol{\sigma}\rangle$ for some bond $(i, i+1)$. We need their $\hat{\mathcal{L}}_0$ eigenvalues to evaluate the denominator in Eq. (5). Computing $\hat{\mathcal{L}}_0\Lambda^{\boldsymbol{\sigma}\boldsymbol{\sigma}'}$, one finds that the eigenvalues are $-\gamma$ or $-\gamma \pm iJ_z$ depending on the values of σ_{i-1}, σ_i ($\sigma_{i+1} = -\sigma_i$), and σ_{i+2}. However, as $\gamma \gg |J_{xy}|, |J_z|$ and one only needs the effective Liouvillian up to first order in $1/\gamma$, the factor $1/(\lambda_0 - \hat{\mathcal{L}}_0)$ in Eq. (5) can for all cases be approximated by $1/\gamma$.

$$\frac{1}{\gamma \pm iJ_z} = \frac{1}{\gamma} + \mathcal{O}(\gamma^{-2})$$

With the terms $h_i := \frac{J_{xy}}{2}(S_i^+ S_{i+1}^- + S_i^- S_{i+1}^+)$ in H_{xy}, the effective Liouvillian attains the form

$$\begin{aligned}\frac{1}{\gamma}\hat{\mathcal{P}}\hat{\mathcal{L}}_1\hat{\mathcal{L}}_1\rho_0^{\boldsymbol{\sigma}} &= -\frac{1}{\gamma}\hat{\mathcal{P}}[H_{xy}, [H_{xy}, \rho_0^{\boldsymbol{\sigma}}]] \\ &= -\frac{1}{\gamma}\sum_i \left(h_i^2 \rho_0^{\boldsymbol{\sigma}} + \rho_0^{\boldsymbol{\sigma}} h_i^2 - 2h_i \rho_0^{\boldsymbol{\sigma}} h_i\right). \end{aligned} \tag{A4}$$

Using that $h_i^2 = \frac{J_{xy}^2}{2}\left(\frac{1}{4} - S_i^z S_{i+1}^z\right)$, one can read off the effective Hamiltonian H_{eff} that describes the action of the effective Liouvillian $\hat{\mathcal{L}}_{\text{eff}}$ on the space $\mathbb{H}$ according to the definition (7). It turns out to be the isotropic Heisenberg ferromagnet with coupling constant J_{xy}^2/γ,

$$H_{\text{eff}} = -\frac{J_{xy}^2}{\gamma}\sum_i \left[\frac{1}{2}(S_i^+ S_{i+1}^- + S_i^- S_{i+1}^+) + S_i^z S_{i+1}^z - \frac{1}{4}\right]. \tag{A5}$$

The spectra of $-\hat{\mathcal{L}}_{\text{eff}}$ and H_{eff} are identical. The gap is decisive for the long-time dynamics and decoherence. To confirm and illustrate the perturbative analysis, we have done an exact diagonalization of the full model $\hat{\mathcal{L}}$ and the effective model $\hat{\mathcal{L}}_{\text{eff}}$. As shown in Table I, with increasing γ, the spectrum of $\hat{\mathcal{L}}_{\text{eff}}$ converges indeed towards the corresponding eigenvalues of $\hat{\mathcal{L}}$. The exact gap of $\hat{\mathcal{L}}_{\text{eff}}$ (finite only for finite system sizes N) is available, because spin waves with the well-known cosine dispersion relation are exact eigenstates of the isotropic Heisenberg ferromagnet (A5).

n	$-\hat{\mathcal{L}}$	$-\hat{\mathcal{L}}_{\text{eff}}$ $\gamma = 100$	$-\hat{\mathcal{L}}_{\text{eff}}$ $\gamma = 10$
0	0	0	0
1	0.292893	0.292877	0.291271
2	0.633975	0.633925	0.629092
3	1.000000	0.999994	0.999369
4	1.707107	1.707042	1.700617
5	2.366025	2.365987	2.362134

Table I: Spectrum of the effective model $\hat{\mathcal{L}}_{\text{eff}}$ [Eq. (A5)] compared to the corresponding eigenvalues of the full Liouvillian [Eq. (A1)] for a XXZ chain of $N = 4$ sites with open boundary conditions, $J_{xy} = 0.5$, and $J_z = 1$. The eigenvalues are given in units of the effective coupling J_{xy}^2/γ.

2. Open transverse Ising model with $L_i = S_i^z$

This appendix presents, in full detail, the perturbation theory for the spin-1/2 Ising model in a transverse field (8) coupled to a Markovian environment according to the Lindblad master equation (1) with $L_i = S_i^z$ and bath coupling strength γ. Using a second order perturbation theory, one can derive an effective Liouville superoperator $\hat{\mathcal{L}}_{\text{eff}}$ for the limit of a weak magnetic field $\gamma \gg |h_x|$. To this purpose, the Liouvillian is split into an unperturbed part $\hat{\mathcal{L}}_0$ and a perturbation $\hat{\mathcal{L}}_1$ such that

$$\hat{\mathcal{L}} = \hat{\mathcal{L}}_0 + \hat{\mathcal{L}}_1, \tag{A6}$$

$$\hat{\mathcal{L}}_0\rho = -i[H_z, \rho] + \gamma\sum_i (S_i^z \rho S_i^z - \rho/4), \tag{A7}$$

$$\hat{\mathcal{L}}_1\rho = -i[H_x, \rho], \tag{A8}$$

where $H_z = 4J_z \sum_i S_i^z S_{i+1}^z$ and $H_x = -2h_x \sum_i S_i^x$ as in Eq. (8).

As in the perturbative analysis of the XXZ model, the steady states (eigenvalue $\lambda_0 = 0$) of the unperturbed part $\hat{\mathcal{L}}_0$ are of the form $\rho_0^{\boldsymbol{\sigma}} := |\boldsymbol{\sigma}\rangle\langle\boldsymbol{\sigma}|$ with $\{S_i^z\}$-eigenstates $|\boldsymbol{\sigma}\rangle$ obeying $S_i^z|\boldsymbol{\sigma}\rangle = \frac{\sigma_i}{2}|\boldsymbol{\sigma}\rangle$. The effective Liouvillian is given by Eq. (5) with $\hat{\mathcal{P}}$ projecting onto the space $\mathbb{H}$ that is spanned by the unperturbed steady states $\rho_0^{\boldsymbol{\sigma}}$. The differences to the calculation for the XXZ model in appendix A 1 are that, here, the total magnetization is not conserved and that the factor $1/(\lambda_0 - \hat{\mathcal{L}}_0)$ in Eq. (5) is now nontrivial. Starting from one of the unperturbed steady states, the intermediate states (after application of $\hat{\mathcal{L}}_1$) are of the form $\Lambda^{\boldsymbol{\sigma}\boldsymbol{\sigma}'} := |\boldsymbol{\sigma}\rangle\langle\boldsymbol{\sigma}'|$ such that $|\boldsymbol{\sigma}'\rangle = 2S_i^x|\boldsymbol{\sigma}\rangle$ for some site i. Computing $\hat{\mathcal{L}}_0\Lambda^{\boldsymbol{\sigma}\boldsymbol{\sigma}'}$, one finds that the $\hat{\mathcal{L}}_0$ eigenvalues of the intermediate states are $-\gamma/2 - i(E_{\boldsymbol{\sigma}} - E_{\boldsymbol{\sigma}'})$. Here, $E_{\boldsymbol{\sigma}} := \langle\boldsymbol{\sigma}|H_z|\boldsymbol{\sigma}\rangle$ and $E_{\boldsymbol{\sigma}} - E_{\boldsymbol{\sigma}'} = 0$ or $\pm 4J_z$ depending on the values of σ_{i-1}, σ_i, and σ_{i+1}. With the definition of the state $|\boldsymbol{\sigma}, i\rangle := 2S_i^x|\boldsymbol{\sigma}\rangle$ and the corresponding eigenvalue of H_z labeled by $E_{\boldsymbol{\sigma}}^i$, the effective Liouvillian (5) takes the form

$$\begin{aligned}\hat{\mathcal{L}}_{\text{eff}}|\boldsymbol{\sigma}\rangle\langle\boldsymbol{\sigma}| &= \hat{\mathcal{P}}\hat{\mathcal{L}}_1\frac{1}{\lambda_0 - \hat{\mathcal{L}}_0}\hat{\mathcal{L}}_1|\boldsymbol{\sigma}\rangle\langle\boldsymbol{\sigma}| \\ &= i\hat{\mathcal{P}}\hat{\mathcal{L}}_1\sum_i\left(\frac{h_x|\boldsymbol{\sigma}, i\rangle\langle\boldsymbol{\sigma}|}{\gamma/2 + i(E_{\boldsymbol{\sigma}}^i - E_{\boldsymbol{\sigma}})} - h.c.\right) \\ &= -\gamma h_x^2\sum_i\frac{|\boldsymbol{\sigma}\rangle\langle\boldsymbol{\sigma}| - |\boldsymbol{\sigma}, i\rangle\langle\boldsymbol{\sigma}, i|}{(\gamma/2)^2 + (E_{\boldsymbol{\sigma}}^i - E_{\boldsymbol{\sigma}})^2}.\end{aligned} \tag{A9}$$

Employing $|E_{\boldsymbol{\sigma}}^i - E_{\boldsymbol{\sigma}}| = 2|J_z(\sigma_{i-1} + \sigma_{i+1})|$, one can read off the effective Hamiltonian H_{eff} that describes the action of the effective Liouvillian $\hat{\mathcal{L}}_{\text{eff}}$ on the space $\mathbb{H}$ according to the definition (7) and finds

$$\begin{aligned}H_{\text{eff}} = &\quad \alpha\sum_i\left(\frac{1}{4} - S_{i-1}^z S_{i+1}^z\right)\left(\frac{1}{2} - S_i^x\right) \\ &+ \alpha'\sum_i\left(\frac{1}{4} + S_{i-1}^z S_{i+1}^z\right)\left(\frac{1}{2} - S_i^x\right) \\ =&\sum_i\left(\frac{\alpha + \alpha'}{4} - (\alpha - \alpha')S_{i-1}^z S_{i+1}^z\right)\left(\frac{1}{2} - S_i^x\right)\end{aligned} \tag{A10}$$

with

$$\alpha = \frac{\gamma(2h_x)^2}{(\gamma/2)^2} \quad\text{and}\quad \alpha' = \frac{\gamma(2h_x)^2}{(\gamma/2)^2 + (4J_z)^2}. \tag{A11}$$

We are particularly interested in the gap (2) of $\hat{\mathcal{L}}_{\text{eff}}$ which is given by that of H_{eff} and determines the decoherence. Let $|\uparrow_i^x\rangle$ and $|\downarrow_i^x\rangle$ denote the normalized eigenstates of S_i^x with eigenvalues $\pm 1/2$. In this notation, the fully polarized state

$$|\psi_0\rangle = |\uparrow^x\uparrow^x\cdots\uparrow^x\rangle \tag{A12}$$

is the eigenstate of H_{eff} with eigenvalue $\lambda_0 = 0$. As H_{eff} is positive-semidefinite ($H_{\text{eff}} \succeq 0$), $|\psi_0\rangle$ is its ground state. Note that the counterpart of $|\psi_0\rangle$ in $\mathbb{H}$ is the maximally mixed state $\mathbb{1} = \sum_{\boldsymbol{\sigma}}|\boldsymbol{\sigma}\rangle\langle\boldsymbol{\sigma}|$ which is also the exact steady state of $\hat{\mathcal{L}}$.

In order to determine or bound the gap, the first intuition may be to flip a single spin, i.e., to consider states

$$|\phi_1^i\rangle := |\uparrow^x\uparrow^x\cdots\uparrow^x\downarrow_i^x\uparrow^x\cdots\uparrow^x\rangle. \tag{A13}$$

They provide the upper bound

$$\langle\phi_1^i|H_{\text{eff}}|\phi_1^i\rangle = \frac{\alpha + \alpha'}{4} \tag{A14}$$

to the gap. The same bound pertains for any superposition of the states $|\phi_1^i\rangle$. One can also construct exact

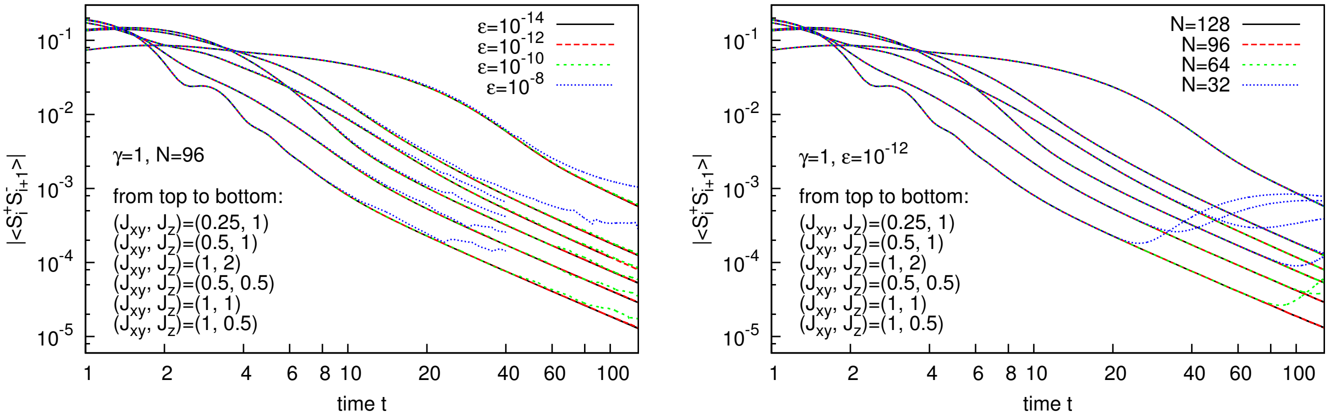

Figure 5: Convergence analysis for the open XXZ model (A1) at the example of the expectation value $\langle S_i^+ S_{i+1}^-\rangle$ with different J_{xy} and J_z, and fixed bath coupling $\gamma = 1$, where site i is in the middle of the chain. Left: variation of the DMRG truncation threshold ϵ for the system size $N = 96$. Right: variation of the system size for the truncation threshold $\epsilon = 10^{-12}$.

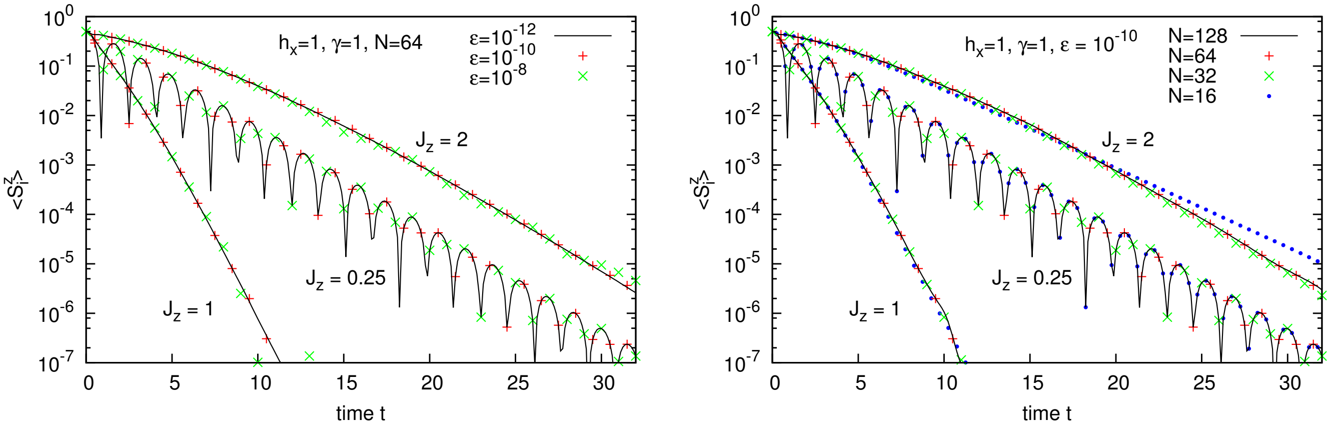

Figure 6: Convergence analysis for the open transverse-field Ising model (A6) at the example of the magnetization $\langle S_i^z\rangle$ with different J_z, fixed bath coupling $\gamma = 1$, and field $h_x = 1$, where site i is in the middle of the chain. Left: variation of the DMRG truncation threshold ϵ for the system size $N = 64$. Right: variation of the system size for the truncation threshold $\epsilon = 10^{-10}$.

spin-wave-type eigenstates $|\tilde{\psi}_1^k\rangle$ where a pair of spin defects is bound and travels through the lattice.

$$|\psi_1^j\rangle := |\uparrow^x\uparrow^x\cdots\uparrow^x\downarrow_j^x\downarrow_{j+1}^x\uparrow^x\cdots\uparrow^x\rangle \tag{A15}$$

$$|\tilde{\psi}_1^k\rangle := N^{-1/2}\sum_j e^{-ikj}|\psi_1^j\rangle \tag{A16}$$

From $H_{\text{eff}}|\psi_1^j\rangle = \frac{\alpha+\alpha'}{2}|\psi_1^j\rangle - \frac{\alpha-\alpha'}{4}(|\psi_1^{j-1}\rangle + |\psi_1^{j+1}\rangle)$ follows the eigenequation

$$H_{\text{eff}}|\tilde{\psi}_1^k\rangle = \left(\frac{\alpha+\alpha'}{2} - \frac{\alpha-\alpha'}{2}\cos(k)\right)|\tilde{\psi}_1^k\rangle. \tag{A17}$$

The minimum eigenvalue α' is obtained for $k = 0$.

Using exact diagonalization (ED), we have asserted that the first excited state is similar to $|\phi_1^i\rangle$ [Eq. (A13)] for $\alpha'/\alpha \simeq 1$ (small J_z) with a gap $\lambda_1 \sim \frac{\alpha+\alpha'}{4}$. For sufficiently small α'/α (sufficiently large J_z), $|\tilde{\psi}_1^k\rangle$ [Eq. (A16)] becomes the first excited state with the gap $\lambda_1 = \alpha'$. In contrast to the open XXZ model discussed in appendix A 1, the gap for the thermodynamic limit is hence finite. Consequently, the coherence decay is always exponential in this model as described in the main text.

Appendix B: One and two spins with $L = S^z$

For completeness and in order to have a consistency check for the the perturbative analysis presented above in appendix A 2, let us shortly discuss the decoherence for a single spin-1/2 in a transverse magnetic field. The Liouville master equation for the Hamiltonian $H = -2h_x S^x$ and the Lindblad operator $L = S^z$ reads

$$\partial_t \rho = i[2h_x S^x, \rho] + \gamma(S^z\rho S^z - \rho/4). \tag{B1}$$

Parameterizing the density, matrix as $\rho = \left[\begin{smallmatrix} a & b+ic \\ b-ic & 1-a \end{smallmatrix}\right]$, we have

$$\partial_t \rho = i h_x \begin{bmatrix} -2ic & 1-2a \\ 2a-1 & 2ic \end{bmatrix} - \frac{\gamma}{2} \begin{bmatrix} 0 & b+ic \\ b-ic & 0 \end{bmatrix},$$

giving the three equations

$$\partial_t a = 2h_x c, \quad \partial_t b = -\frac{\gamma}{2} b, \quad \partial_t c = h_x(1-2a) - \frac{\gamma}{2} c.$$

So b decays as $b(t) = b(0)e^{-\gamma t/2}$. The first and third equations imply $\partial_t^2 c = -4h_x^2 c - \frac{\gamma}{2}\partial_t c$ with the solution $c(t) = c_+ e^{i\omega_+ t} + c_- e^{i\omega_- t} + c.c.$ and

$$\omega_\pm = \frac{i\gamma}{4} \pm \sqrt{4h_x^2 - \left(\frac{\gamma}{4}\right)^2}. \tag{B2}$$

For $\gamma \leq 8|h_x|$, the coherence hence decays in the long-time limit as $\sim e^{-\gamma t/4}$. For large γ however ($\gamma > 8|h_x|$), the square root in Eq. (B2) becomes imaginary and, thus, alters the decoherence rate from $\gamma/4$ to $\gamma/4 - \sqrt{(\gamma/4)^2 - 4h_x^2} = 8h_x^2/\gamma + \mathcal{O}(h_x^4/\gamma^3)$. This can be compared with the perturbative upper bound $(\alpha + \alpha')/4$ [Eq. (A14)] for the gap of the transverse-field Ising model as derived in appendix A 2. For $J_z = 0$, this bound has indeed the same value found here, $(\alpha+\alpha')/4 = 8h_x^2/\gamma$. So the two computations are consistent.

In the main text, we also mention the decoherence for two spins with zero total magnetization ($S_1^z + S_2^z = 0$) evolving according to the Lindblad master equation with the XXZ interaction $H' = \frac{J_{xy}}{2}(S_1^+ S_2^- + S_1^- S_2^+) + J_z S_1^z S_2^z$ and the dissipative term $\hat{\mathcal{D}}'\rho' = \gamma'(S_1^z \rho' S_1^z + S_2^z \rho' S_2^z - \rho'/2)$. This model maps to the single spin in a transverse field (B1) if we associate the state $|\uparrow\downarrow\rangle$ with the spin-up state, and $|\downarrow\uparrow\rangle$ with the spin-down state. The resulting single-spin dynamics is governed by the Hamiltonian $H = J_{xy}S^x - J_z/4$ and the dissipative term $\hat{\mathcal{D}}\rho = 2\gamma'(S^z\rho S^z - \rho/4)$. So the equation of motion is just Eq. (B1) with transverse field $h_x = -J_{xy}/2$ and bath coupling $\gamma = 2\gamma'$. Hence, for $\gamma' \leq 2|J_{xy}|$, the decoherence rate is $\gamma'/2$. As is shown in the main part of the paper, the decoherence changes from this exponential behavior to a power-law decay in the thermodynamic limit of the corresponding many-particle system.

Appendix C: Convergence of the tDMRG results

The numerical investigations are based on the time-dependent density matrix renormalization group (tDMRG) [26–28]. We use a Trotter-Suzuki decomposition of the propagator $\exp(\hat{\mathcal{L}}t)$ [34] for which the error is of fifth order in the time-step $\Delta t = 0.125$. As described in the main text, an essential part of the algorithm is to truncate small-weight components in the singular value decomposition of the density matrix $\rho(t)$. This is necessary in order to bound the computation cost. The corresponding truncation threshold ϵ determines the accuracy and the computation cost of the simulation. One has to ensure convergence of the numerical results with respect to ϵ and with respect to the system size N, as we are interested in the physics of the thermodynamic limit $N \to \infty$.

Figure 5 shows the analysis for the dissipative XXZ model (A1). The results are sufficiently converged for a truncation threshold of $\epsilon = 10^{-12}$ and the system size $N = 96$. The simulations presented in the main text were done with these parameters. Figure 6 shows the analysis for the dissipative transverse-field Ising model (A6). A truncation threshold of $\epsilon = 10^{-10}$ and the system size $N = 64$ are sufficient and were used for the simulations presented in the main text.

[1] U. Weiss, *Quantum Dissipative Systems*, 2nd ed. (World Scientific, Singapore, 1999).

[2] H.-P. Breuer and F. Petruccione, *The Theory of Open Quantum Systems* (Oxford University Press, Oxford, 2007).

[3] C. W. Gardiner and P. Zoller, *Quantum noise*, 3rd ed. (Springer, Berlin, 2004), p. 449.

[4] M. A. Cazalilla, F. Sols, and F. Guinea, Phys. Rev. Lett. **97**, 076401 (2006).

[5] T. Prosen and I. Pižorn, Phys. Rev. Lett. **101**, 105701 (2008).

[6] A. J. Daley, J. M. Taylor, S. Diehl, M. Baranov, and P. Zoller, Phys. Rev. Lett. **102**, 040402 (2009).

[7] S. Diehl, A. Tomadin, A. Micheli, R. Fazio, and P. Zoller, Phys. Rev. Lett. **105**, 015702 (2010).

[8] E. G. Dalla Torre, E. Demler, T. Giamarchi, and E. Altman, Nature Phys. **6**, 806 (2010).

[9] T. Prosen, Phys. Rev. Lett. **107**, 137201 (2011).

[10] H. Schwager, J. I. Cirac, and G. Giedke, Phys. Rev. A **87**, 022110 (2013).

[11] D. Poletti, J.-S. Bernier, A. Georges, and C. Kollath, Phys. Rev. Lett. **109**, 045302 (2012).

[12] D. Poletti, P. Barmettler, A. Georges, and C. Kollath, arXiv:1212.4637 (2012).

[13] J.-S. Bernier, P. Barmettler, D. Poletti, and C. Kollath, arxiv:1211.4087 (2012).

[14] M. Höning, M. Moos, and M. Fleischhauer, Phys. Rev. A **86**, 013606 (2012).

[15] D. Golež, J. Bonča, L. Vidmar, and S. A. Trugman, Phys. Rev. Lett. **109**, 236402 (2012).

[16] B. Horstmann, J. I. Cirac, and G. Giedke, Phys. Rev. A **87**, 012108 (2013).

[17] J. J. Mendoza-Arenas, T. Grujic, D. Jaksch, and S. R. Clark, arXiv:1302.5629 (2013).

[18] C. Cormick, A. Bermudez, S. F. Huelga, and M. B. Plenio, arXiv:1304.2201 (2013).

[19] J. T. Barreiro, P. Schindler, O. Gühne, T. Monz, M. Chwalla, C. F. Roos, M. Hennrich, and R. Blatt, Nature

Phys. **6**, 943 (2010).

[20] J. T. Barreiro, M. Müller, P. Schindler, D. Nigg, T. Monz, M. Chwalla, M. Hennrich, C. F. Roos, P. Zoller, and R. Blatt, Nature **470**, 486 (2011).

[21] P. Schindler, M. Müller, D. Nigg, J. T. Barreiro, E. A. Martinez, M. Hennrich, T. Monz, S. Diehl, P. Zoller, and R. Blatt, arXiv:1212.2418 (2012).

[22] S. Diehl, A. Micheli, A. Kantian, B. Kraus, H. Büchler, and P. Zoller, Nature Phys **4**, 878 (2008).

[23] F. Verstraete, M. M. Wolf, and J. Cirac, Nature Phys **5**, 633 (2009).

[24] S. Diehl, W. Yi, A. J. Daley, and P. Zoller, Phys. Rev. Lett. **105**, 227001 (2010).

[25] S. Diehl, E. Rico, M. A. Baranov, and P. Zoller, Nature Phys **7**, 971 (2011).

[26] G. Vidal, Phys. Rev. Lett. **93**, 040502 (2004).

[27] S. R. White and A. E. Feiguin, Phys. Rev. Lett. **93**, 076401 (2004).

[28] A. J. Daley, C. Kollath, U. Schollwöck, and G. Vidal, J. Stat. Mech P04005 (2005).

[29] G. Lindblad, Commun. Math. Phys. **48**, 119 (1976).

[30] A. J. Leggett, S. Chakravarty, A. T. Dorsey, M. P. A. Fisher, A. Garg, and W. Zwerger, Rev. Mod. Phys. **59**, 1 (1987).

[31] P. Barmettler, M. Punk, V. Gritsev, E. Demler, and E. Altman, Phys. Rev. Lett. **102**, 130603 (2009).

[32] P. Barmettler, M. Punk, V. Gritsev, E. Demler, and E. Altman, New J. Phys **12**, 055017 (2010).

[33] T. Barthel, C. Kasztelan, I. P. McCulloch, and U. Schollwöck, Phys. Rev. A **79**, 053627 (2009).

[34] M. Kliesch, T. Barthel, C. Gogolin, M. Kastoryano, and J. Eisert, Phys. Rev. Lett. **107**, 120501 (2011).

[35] L. Accardi, Phys. Rep. **77**, 169 (1981).

[36] M. Fannes, B. Nachtergaele, and R. F. Werner, J. Phys. A: Math. Gen. **24**, L185 (1991).

[37] S. Rommer and S. Östlund, Phys. Rev. B **55**, 2164 (1997).

[38] D. P. DiVincenzo, Fortschr. Phys. **48**, 771 (2000).

[39] T. D. Ladd, F. Jelezko, R. Laflamme, Y. Nakamura, C. Monroe, and J. L. O'Brien, Nature **464**, (2010).

[40] J. E. Mooij, T. P. Orlando, L. Levitov, L. Tian, C. H. van der Wal, and S. Lloyd, Science **285**, 1036 (1999).

[41] F. Yoshihara, K. Harrabi, A. O. Niskanen, Y. Nakamura, and J. S. Tsai, Phys. Rev. Lett. **97**, 167001 (2006).

[42] J. Clarke and F. K. Wilhelm, Nature **453**, (2008).

[43] J. B. Majer, F. G. Paauw, A. C. J. ter Haar, C. J. P. M. Harmans, and J. E. Mooij, Phys. Rev. Lett. **94**, 090501 (2005).

[44] M. W. Johnson, M. H. S. Amin, S. Gildert, T. Lanting, F. Hamze, N. Dickson, R.Harris, A. J. Berkley, J. Johansson, P. Bunyk, E. M. Chapple, C. Enderud, J. P. Hilton, K. Karimi, E. Ladizinsky, N. Ladizinsky, T. Oh, I. Perminov, C. Rich, M. C. Thom, E. Tolkacheva, C. J. S. Truncik, S. Uchaikin, J. Wang, B.Wilson, and G. Rose, Nature **473**, 194 (2011).

[45] M. J. Storcz and F. K. Wilhelm, Phys. Rev. A **67**, 042319 (2003).

[46] I. Bloch, J. Dalibard, and W. Zwerger, Rev. Mod. Phys. **80**, 885 (2008).

[47] J. Anglin, Phys. Rev. Lett. **79**, 6 (1997).

[48] F. Gerbier and Y. Castin, Phys. Rev. A **82**, 013615 (2010).

[49] H. Pichler, A. J. Daley, and P. Zoller, Phys. Rev. A **82**, 063605 (2010).

[50] D. Loss and D. P. DiVincenzo, Phys. Rev. A **57**, 120 (1998).

[51] R. Hanson, L. P. Kouwenhoven, J. R. Petta, S. Tarucha, and L. M. K. Vandersypen, Rev. Mod. Phys. **79**, 1217 (2007).

[52] M. D. Shulman, O. E. Dial, S. P. Harvey, H. Bluhm, V. Umansky, and A. Yacoby, Science **336**, 202 (2012).